

# Ultra-Sensitivity Glucose Sensor Based on Field Emitters

Huibiao Liu · Xuemin Qian · Shu Wang ·  
Yuliang Li · Yinglin Song · Daoben Zhu

Received: 4 May 2009 / Accepted: 2 June 2009 / Published online: 14 June 2009  
© to the authors 2009

**Abstract** A new glucose sensor based on field emitter of ZnO nanorod arrays (ZNA) was fabricated. This new type of ZNA field emitter-based sensor shows high sensitivity with experimental limit of detection of 1 nM glucose solution and a detection range from 1 nM to 50  $\mu$ M in air at room temperature, which is lower than that of glucose sensors based on surface plasmon resonance spectroscopy, fluorescence signal transmission, and electrochemical signal transduction. The new glucose sensor provides a key technique for promising consuming application in biological system for detecting low levels of glucose on single cells or bacterial cultures.

**Keywords** ZnO nanorod arrays · Glucose sensor · Field emitter · High sensitivity

---

H. Liu (✉) · X. Qian · S. Wang · Y. Li · D. Zhu  
CAS Key Laboratory of Organic Solid, Beijing National  
Laboratory for Molecular Sciences (BNLMS), Institute of  
Chemistry, Chinese Academy of Sciences, 100190 Beijing,  
People's Republic of China  
e-mail: liuhb@iccas.ac.cn

X. Qian  
e-mail: qianxuemin1813@sina.com

S. Wang  
e-mail: wangshu@iccas.ac.cn

Y. Li  
e-mail: ylli@iccas.ac.cn

D. Zhu  
e-mail: dbzhu@iccas.ac.cn

X. Qian · Y. Song  
School of Physical Science and Technology, Suzhou University,  
215006 Suzhou, Jiangsu, People's Republic of China

Y. Song  
e-mail: ylsong@hit.edu.cn

## Introduction

The glucose sensors are becoming an increasingly active area of research due to their applications in biological, chemical analyze, and clinical detection [1]. Many glucose sensors based on surface plasmon resonance (SPR) spectroscopy [2, 3], fluorescence signal transmission (FST) [4–8], and electrochemical signal transduction (EST) [9–11], have been reported. However, the sensitivity of these glucose sensors was mostly confined to the millimolar, which restricted their application in the case of lower glucose concentration, such as cellular signal transduction and protein biosynthesis in single cell or bacterial cultures. In order to further promote the sensitivity, intensive efforts have been made in the exploration of a glucose sensors based on nanostructured materials such as carbon nanotubes, semiconductor quantum dots, and nanowires [12–16].

Due to their unique properties of good biological compatibility and stability, nanomaterials of metal oxides could play an important role in adsorption of biomolecules. They are able to couple with different redox enzymes, which make them particular promising for their applications on biosensors and bioelectronics [17, 18]. Being an important n-type semiconductor with a wide band gap (3.37 eV), ZnO possesses many versatile properties: high optical transparency, semiconducting, piezoelectric, nontoxicity, chemical stability, and electrochemical activity. Recently, one dimensional (1D) ZnO nanostructures for nanodevices such as field emitter [19], nanopiezotronics [20], gas and pH sensor [21], biosensor [22], transistor [23], and temperature laser [24], have received more and more attention due to their distinguished performance, high specific surface area, and facile preparation. 1D ZnO nanostructures have been used as electron mediators and adsorption matrices in amperometric biosensors [22]. Sun et al.

[22, 25, 26] constructed a glucose amperometric biosensor using 1D ZnO nanostructures as supporting materials for glucose oxidase ( $\text{GO}_x$ ) loading, whose detection limit measured was 0.02 and 0.01 mM. Ren et al. [27] fabricated a ZnO nanorod-gated AlGa/GaN high electron mobility transistor for the detection of glucose, which showed a linear range from 0.01 to 3.45 mM. In this contribution, we present a new type of nanodevice, a glucose sensor based on field emitter of ZnO nanorod arrays (ZNA). The obvious changes of field emission properties of ZNA caused by surface energy band bending, which induced by surface adsorptions. This new ZNA field emitter-based sensor shows high sensitivity with an experimental limit of detection (LOD) of 1 nM glucose solution and a wide detection range from 1 nM to 50  $\mu\text{M}$  in air at room temperature, which is lower than that of glucose sensor based on FST and EST.

## Experimental Details

### Materials and Apparatus

$\text{GO}_x$  (100 U  $\text{mg}^{-1}$ ) was purchased from Amersco Inc. (USA). All other reagents (analytical-grade) were purchased from Beijing Chemical Reagent Company. The buffer solution was phosphate buffer (6 mM, pH 7.4). The water was purified using a Millipore filtration system.

The arrays of ZNA are characterized by field emission scanning electron microscopy (FESEM, Hitachi, S-4300). The field emission properties of ZNA are measured using a two-parallel-plate configuration in a homemade vacuum chamber at a base pressure of  $\sim 1.0 \times 10^{-6}$  Pa at room temperature. The sample is attached to one of stainless-steel plates as cathode with the other plate as anode. The distance between the electrodes is 300  $\mu\text{m}$ . A direct current voltage sweeping from 0 to 5,000 V was applied to the sample at a step of 50 V. The emission current is monitored using a Keithley 6485 picoammeter.

### Synthesis of ZNA and Glucose Sensors

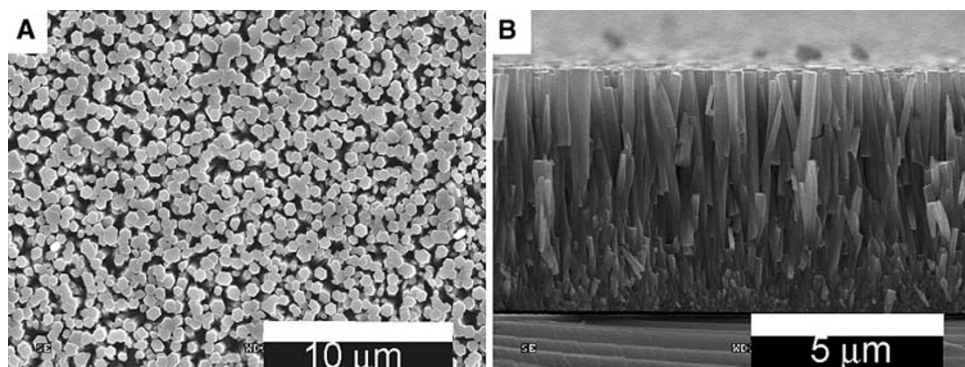
ZNA were directly grown on a Si (100) wafer with an area of 4  $\text{cm}^2$  by a multi-step hydrothermal process [28]. The Si (100) wafer (4  $\text{cm}^2$ ) is equally cut as 16 pieces of same area (0.5  $\times$  0.5  $\text{cm}^2$ ) samples. The samples for measurement of field emission were then prepared as follow: the films of Si (100) wafers deposited with ZNA were immersed in 2 mL Eppendorf cups with 10  $\mu\text{L}$  of glucose oxidase ( $\text{GO}_x$ ) (10 U  $\mu\text{L}^{-1}$ ) and 1 mL of PBS buffer solution, respectively. Then the  $\beta\text{-D-(+)}$  glucose with different concentrations (from 1 nM to 50  $\mu\text{M}$ ) was added into the solution and incubated for 30 min at room temperature. After incubation, the samples were washed by pure water for three times. The samples were desiccated via vacuum for field emission measurement.

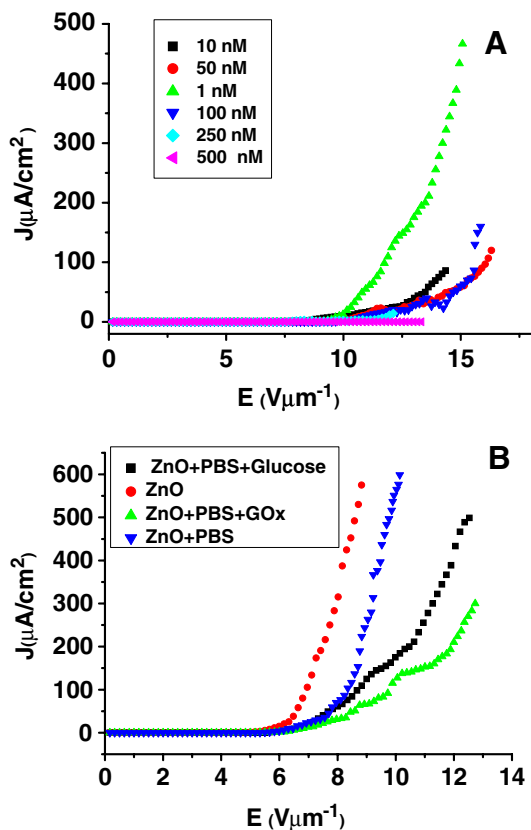
## Results and Discussion

Figure 1a shows a typical SEM image of the as-grown ZNA prepared through hydrothermal process, which presents a rodlike morphology with a hexagonal cross-section. The nanorods are uniform on size with an average diameter of about  $500 \pm 10$  nm. The cross-section of SEM image (Fig. 1b) demonstrates the nanorods are aligned along the perpendicular direction of the Si (100) wafer. The length of nanorods is about 6  $\mu\text{m}$ .

The field emission properties of the pure ZNA and ZNA film immersed with different concentrations glucose in PBS buffer solution are illustrated in Figs. 2a, b. As shown in Fig. 2a, the turn on field ( $E_{\text{to}}$ ) of the film of pure ZNA is  $5.83 \text{ V } \mu\text{m}^{-1}$ . The  $E_{\text{to}}$  values of ZNA immersed with 1, 10, 50, 100, and 250 nM glucose solution are 9.82, 9.96, 10.8, 10.97, 11.95  $\text{V } \mu\text{m}^{-1}$ , respectively. The control experiments show that the  $E_{\text{to}}$  values of ZNA immersing in PBS buffer solution, the glucose solution in PBS and the  $\text{GO}_x$  solution in PBS and are 6.47, 6.5, and 6.83  $\text{V } \mu\text{m}^{-1}$ , respectively (Fig. 2b). These values are slightly bigger than

**Fig. 1** SEM images of ZNA: **a** Top view, **b** cross-section view





**Fig. 2** Field emission J–E curves **a** the ZNA immersing in the glucose concentration from 1 to 500 nM in 6 mM PBS buffer solution and 10 U  $\mu\text{L}^{-1}$  glucose oxidase with a pH value of 5.8. **b** The control experiments, the ZNA immersing 6 mM PBS buffer solution, 1 mM glucose in 6 mM PBS buffer solution, 10 U  $\mu\text{L}^{-1}$  glucose oxidase in 6 mM PBS buffer solution, respectively, with a pH value of 5.8

that of pure ZNA. The  $E_{\text{to}}$  value of ZNA film immersed in 1 nM glucose solution increases obviously to  $9.82 \text{ V } \mu\text{m}^{-1}$ , which is easily distinguished in comparison with that of pure ZNA ( $5.83 \text{ V } \mu\text{m}^{-1}$ ). However, the measurement of field emission properties on the film of ZNA indicating no any signal was observed when the glucose concentration increased to 500 nM. This indicates that the experimental LOD is 1 nM, which is much lower compared with the glucose sensors based on GaN/AlGaN high electron mobility transistors [27].

Figure 3a shows the R–M curve of the ZNA field emitters in different concentrations of 1 nM–50  $\mu\text{M}$  glucose in PBS buffer and  $\text{GO}_x$  solutions. It is clearly observed that the resistance of ZNA field emitter increases promptly with the increase of the glucose concentration. The resistance of the pure ZNA is about  $650 \text{ } \Omega$ , which raises 9.3 times in the presence of 1 nM glucose ( $6,000 \text{ } \Omega$ ) and about 12 times for 10 nM concentration of glucose ( $8,000 \text{ } \Omega$ ). When the glucose concentration increases to 50  $\mu\text{M}$ , the resistance is about 420 times that of the pure ZNA. However, the resistances of the ZNA in control experiments

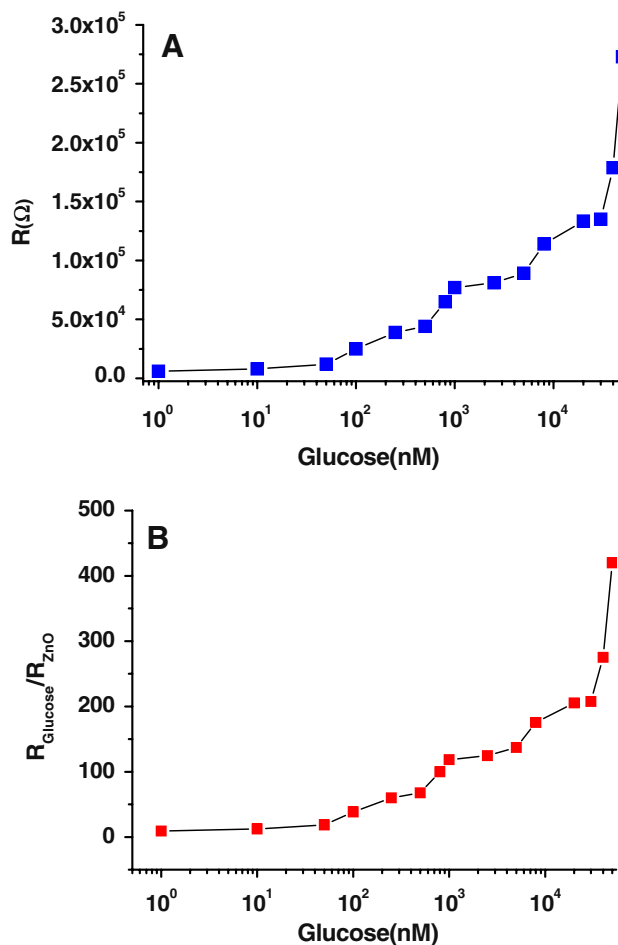
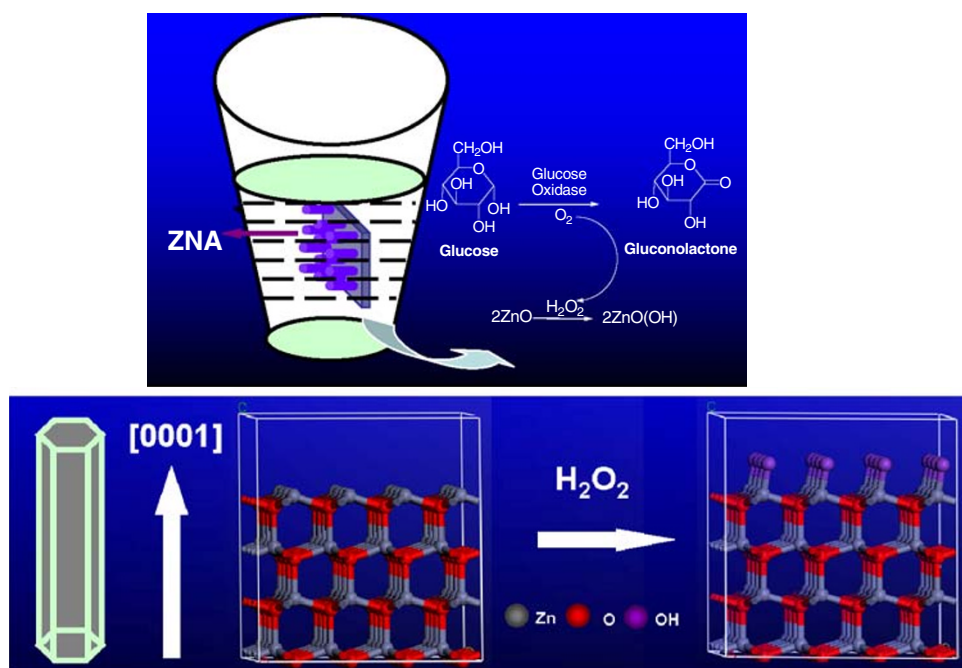


**Fig. 3** **a** Plot of change resistance ( $R$ ) as a function of concentrations ( $M$ ) from 1 nM to 50  $\mu\text{M}$  in 6 mM PBS buffer solution and 10 U  $\mu\text{L}^{-1}$  glucose oxidase with a pH value of 5.8. **b** Dependence relation between response sensitivity and glucose concentrations

only increase slightly. Obviously,  $\text{H}_2\text{O}_2$  that generated from the oxidation of glucose by the  $\text{GO}_x$  catalyzed (Fig. 4) has strongly influence on the field emission property and conductivity of the ZNA. The ratio of  $R_{\text{glucose}}/R_{\text{ZnO}}$  for the ZNA field emitter-based glucose sensor presents a good dependence on the glucose concentrations (Fig. 3b). At this point, our ZNA field emitter-based glucose sensor surpasses previous glucose sensors based on many oxide semiconductors [22, 25–27, 29].

The properties of ZnO nanostructures are significantly influenced by surface adsorptions, which have been attracting great attention because the surface absorptions sometime disturb the fluorescence, field emission, and field effect transistors [30–32]. In general, the changes of properties caused by surface energy band bending, induced by surface adsorptions. As shown in Fig. 4,  $\text{GO}_x$  specifically catalyzes the oxidation of  $\beta\text{-D-(+)-glucose}$  into gluconate and  $\text{H}_2\text{O}_2$ .  $\text{H}_2\text{O}_2$  and ZnO to form  $\text{ZnO}(\text{OH})_x$  on the surface of ZnO nanorods [25], which depletes the electrons

**Fig. 4** A schematic illustration of the ZNA field emitter-based glucose sensor operating principles



on the ZnO nanorods and yields oxygen ions ( $O^-$ ,  $O^{2-}$ , or  $O_2^-$ ) [33]. Leading to the electrons on the ZnO nanorods are trapped by the adsorbed oxygen molecules, and the surface depletion region of ZnO nanorods can be formed, making resistance increase. While the  $H_2O_2$  is raised with the increase of glucose, more electrons are captured by the oxygen molecules at the nanorod surface. Thus, the surface depletion region is widened and the carrier density in the ZnO nanorod is decreased even more. At the same time, gluconolactone can be absorbed strongly on the surface of ZnO nanorods by hydrogen bonding with  $ZnO(OH)_x$ , which induces the surface passivation to block the electrons emission of ZnO nanorods under electronic field. The surface passivation increases to completely deplete the electrons emission of ZnO nanorods with the increase of  $ZnO(OH)_x$  on the surface of ZnO nanorods. The result indicates that field emission properties were not observed on the ZNA at the glucose concentration  $\geq 500$  nM.

## Conclusions

In summary, we demonstrated a new glucose sensor based on the field emitter of ZNA. The results showed that a wide range of glucose concentrations from 1 nM to 50  $\mu$ M is easily detected, which exhibits ultra-sensitivity for glucose detection. The experimental LOD of glucose concentration is 1 nM, which is lower than previous reported glucose sensor based on EST, FST, and SPR. The new glucose sensor shows the potential to detect low levels of glucose in biological system.

**Acknowledgments** This work was supported by the National Nature Science Foundation of China (10874187 and 20873155) and the National Basic Research 973 Program of China.

## References

1. N.A. Rakow, K.S. Suslick, *Nature* **406**, 710 (2000)
2. B. Lee, V.H. Perez-Luna, *Anal. Chem.* **77**, 7204 (2005)
3. K. Aslan, J.R. Lakowicz, C.D. Geddes, *Anal. Chem.* **77**, 2007 (2005)
4. X.-D. Ge, L. Tolosa, G. Rao, *Anal. Chem.* **76**, 1403 (2004)
5. D.L. Meadows, J.S. Schultz, *Talanta* **35**, 145 (1988)
6. G. Blagoi, N. Rosenzweig, Z. Rosenzweig, *Anal. Chem.* **77**, 393 (2005)
7. F. He, Y. Tang, M. Yu, S. Wang, Y. Li, D. Zhu, *Adv. Funct. Mater.* **16**, 91 (2006)
8. F. He, F. Feng, S. Wang, Y. Li, D. Zhu, *J. Mater. Chem.* **17**, 3702 (2007)
9. W. Chen, H. Yao, C.H. Tzang, J. Zhu, M. Yang, S.-T. Lee, *Appl. Phys. Lett.* **88**, 213104 (2006)
10. T. Chen, K.A. Friedman, I. Lei, A. Heller, *Anal. Chem.* **72**, 3757 (2000)
11. A.G. Sapre, A. Bedekar, A.V. Deshpande, A.M. Lali, *Biotechnol. Lett.* **22**, 569 (2000)
12. J. Wang, M. Musameh, Y.H. Lin, *J. Am. Chem. Soc.* **125**, 2408 (2003)
13. H.D. Duong, J. Il Rhee, *Talanta* **73**, 899 (2007)
14. M. Curreli, C. Li, Y.H. Sun, B. Lei, M.A. Gundersen, M.E. Thompson, C.W. Zhou, *J. Am. Chem. Soc.* **127**, 6922 (2005)
15. Y. Liu, M. Wang, F. Zhao, Z. Xu, S. Dong, *Biosens. Bioelectron.* **21**, 984 (2005)
16. J.I. Yeh, A. Lazareck, J. Ho Kim, J. Xu, S. Du, *Biosens. Bioelectron.* **23**, 568 (2007)
17. E. Topoglidis, A.E.G. Cass, B. O'Regan, J.R. Durrant, *J. Electroanal. Chem.* **517**, 20 (2001)
18. Y.H. Yang, H.F. Yang, M.H. Yang, Y.L. Liu, G.L. Shen, R.Q. Yu, *Anal. Chim. Acta.* **525**, 213 (2004)

19. C.X. Xu, X.W. Sun, *Appl. Phys. Lett.* **83**, 3806 (2003)
20. Z.L. Wang, J.H. Song, *Science* **312**, 242 (2006)
21. H.T. Wang, B.S. Kang, F. Ren, L.C. Tien, P.W. Sadik, D.P. Norton, S.J. Pearton, J. Lin, *J. Appl. Phys. Lett.* **86**, 243503 (2005)
22. J.X. Wang, X.W. Sun, A. Wei, Y. Lei, X.P. Cai, C.M. Li, Z.L. Dong, *Appl. Phys. Lett.* **88**, 233106 (2006)
23. Z.Y. Fan, J.G. Lu, *Appl. Phys. Lett.* **86**, 123510 (2005)
24. X.W. Sun, S.F. Yu, C.X. Xu, C. Yuen, B.J. Chen, S. Li, *Jpn. J. Appl. Phys. 2.* **42**, L1229 (2003)
25. A. Wei, X.W. Sun, J.X. Wang, Y. Lei, X.P. Cai, C.M. Li, Z.L. Dong, W. Huang, *Appl. Phys. Lett.* **89**, 123902 (2006)
26. J. Zang, C.M. Li, X. Cui, J.X. Wang, X.W. Sun, H. Dong, *C.Q. Sun, Electroanalysis* **19**, 1008 (2007)
27. B.S. Kang, H.T. Wang, F. Rena, S.J. Pearton, T.E. Morey, D.M. Dennis, J.W. Johnson, P. Rajagopal, J.C. Roberts, E.L. Piner, K.J. Linthicum, *Appl. Phys. Lett.* **91**, 252103 (2007)
28. L.E. Greene, M. Law, J. Goldberger, F. Kim, J.C. Johnson, Y.F. Zhang, R.J. Saykally, P.D. Yang, *Angew. Chem. Int. Ed.* **42**, 3031 (2003)
29. S.J. Bao, C.M. Li, J.F. Zang, X.Q. Cui, Y. Qiao, J. Guo, *Adv. Funct. Mater.* **18**, 591 (2008)
30. D.S. Bohle, C.J. Spina, *J. Am. Chem. Soc.* **129**, 12380 (2007)
31. Y. Zhang, A. Kolmakov, S. Chretien, H. Metiu, M. Moskovits, *Nano Lett.* **4**, 403 (2004)
32. S. Song, W.K. Hong, S.S. Kwon, T. Lee, *Appl. Phys. Lett.* **92**, 263109 (2008)
33. Q.H. Li, Y.X. Liang, Q. Wan, T.H. Wang, *Appl. Phys. Lett.* **85**, 6389 (2004)